Spontaneous Splitting of a Quadruply Charged Vortex

T. Isoshima,[1] M. Okano,[1] H. Yasuda,[1] K. Kasa,[1] J. A. M. Huhtamäki,[2] M. Kumakura,[3,4] and Y. Takahashi[1,5]

[1]*Department of Physics, Graduate School of Science, Kyoto University, Kyoto 606-8502, Japan*
[2]*Laboratory of Physics, Helsinki University of Technology, P. O. Box 4100, FI-02015 TKK, Finland*
[3]*Graduate School of Engineering, University of Fukui, Bunkyo, Fukui 910-8507, Japan*
[4]*PRESTO, JST, 4-1-8 Honcho Kawaguchi, Saitama 332-0012, Japan*
[5]*CREST, JST, 4-1-8 Honcho Kawaguchi, Saitama 332-0012, Japan*

(Received 7 December 2006; published 14 November 2007)

We studied the splitting instability of a quadruply charged vortex both experimentally and theoretically. The density defect, which is a signature of the vortex core, is experimentally observed to deform into a linear shape. The deformed defect is theoretically confirmed to be an array of four linearly aligned singly charged vortices. The array of vortices rotates and precesses simultaneously with different angular velocities. The initial state of the system is not rotationally symmetric, which enables spontaneous splitting without external perturbations.

DOI: 10.1103/PhysRevLett.99.200403 PACS numbers: 03.75.Lm, 03.75.Kk, 03.75.Mn

Vortices are often observed in classical gases and fluids such as air and water, and they are especially important for understanding the rotational motions of these systems. In quantum fluids and gases, the circulation associated with the vortices is quantized [1]. The concept of a quantized vortex naturally includes both singly and multiply charged vortices. The phase of the order parameter changes by 2π (multiple of 2π) around a singly (multiply) charged vortex line. Singly charged vortices have been found in, e.g., superfluid He [2], superconductors, and condensates of atomic gases [3,4]. Although multiply charged vortices were found in systems of superfluid He [5] and superconductors [6] and studied theoretically [7], it is difficult to experimentally observe their dynamics in these systems. Studies of atomic gases have changed this situation remarkably. Recently several groups have succeeded in creating multiply charged vortices in atomic gases by flipping of a magnetic field [8–10] and by using a Laguerre-Gaussian laser beam [11]. Dilute atomic Bose-Einstein condensates (BECs) are the first systems where we can directly observe the dynamics of multiply charged vortices, the details of which still remain unknown.

The energy of one j-charged vortex is roughly proportional to j^2, which is larger than that of j singly charged vortices [12]. Therefore, except for the case of a nonharmonic and rotated confinement potential where a giant vortex state is energetically preferred [13], multiply charged vortices are energetically unstable and should split into singly charged vortices. Nevertheless, in the first experimental observation of doubly charged vortices in atomic gases where a harmonic and nonrotated trap potential was used, the vortices did not show any sign of splitting [8]. Based on a pioneering study [14] on the stability of a multiply charged vortex, we proposed [15] that the splitting starts from several places in an axially elongated system and the split vortices intertwine. Because of the intertwining, an individual vortex was not clearly observed in the axially integrated image of the atom density. A split vortex was observed in the later experiment [9] and the splitting time was measured as a function of the peak linear density of the condensate. Two independent studies [16,17] successfully reproduced the measured splitting times. In both simulations, the local initiation of the splitting and the intertwining of the split vortices were also observed.

While a doubly charged vortex merely splits into two vortices, a quadruply charged vortex has various patterns of splitting. Splitting patterns of two-, three-, and fourfold rotational symmetries are presented in Ref. [18]. Here we note the role of conservation of angular momentum in the instability of a quadruply charged vortex. Let us assume a radially trapped 2D condensate and its density $n(r)$ is a function of the radius. This simplified model represents the slices of a cigar-shaped condensate. When there is a singly charged vortex at a radius r_i, the angular momentum of the condensate becomes $L_i = 2\pi\hbar \int_{r_i}^{\infty} rn(r)dr$, which is proportional to the number of atoms outside the radius r_i. When a system has four vortices at radii $r_i (i = 1, \ldots, 4)$, the total angular momentum is given by the sum $L = \sum_{i=1}^{4} L_i$. If we consider the conservation of angular momentum only for the sum L, the positions r_i of the vortices are restricted. For example, when the ith vortex goes outward, L_i decreases, and to compensate this another (jth) vortex must go inward and increase L_j. Figure 1 explains this argument schematically. Our initial state is a quadruply charged vortex at radius r_{init}, and therefore $r_i = r_{\text{init}}$ at the beginning. When $r_{\text{init}} = 0$, the splitting of vortices always accompanies decrease of the sum L and thus all r_i should remain zero for the sum L to be conserved. Note that we ignored an additional angular momentum due to surface oscillation of the condensate in this model. In fact, several Bogoliubov excitations include a pair of eigenfunctions that correspond to the vortex splitting and surface excitation, respectively, and small perturbation to the initial state should be enough to split the vortices even right in the

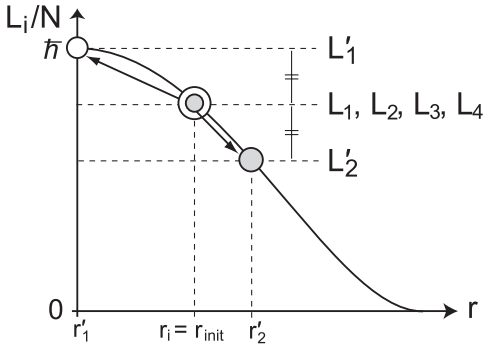

FIG. 1. Schematic plot of conservation of angular momentum. The curve shows the angular momentum L_i as a function of the vortex position r_i. Initially a quadruply charged vortex is at radius r_{init}. After the splitting, two of the vortices, represented by open and solid circles, move to r'_1 and r'_2, for example. In this process, the total angular momentum $L = \sum L_i$ must be conserved. Therefore, if $r'_1 < r_{\text{init}}$, then $r'_2 > r_{\text{init}}$.

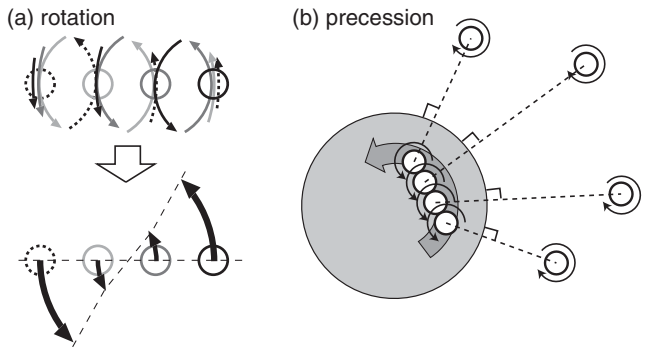

FIG. 2. Schematic plots of vortex dynamics after the splitting. (a) There are four vortices (circles) in the condensate. Sum of the velocity fields (arrows) of each of the vortices results in rotation of the array. (b) The gray area is the condensate. For each of the vortices in the condensate, an antivortex outside the condensate is considered as an image vortex. The original vortices (image vortices) are shown with small circles with counterclockwise (clockwise) arrows. The velocity field of the antivortices makes the original vortices precess as a whole (gray arrow).

center [14,18] within the conservation of angular momentum. However, the aforementioned simplified model still leads us to expect that the off-centered initial position enables a faster and wider splitting as the initial displacement increases without further perturbation.

In this Letter we study the splitting instability of a quadruply charged vortex both experimentally and theoretically. The topologically created quadruply charged vortex was detected as a density defect which is a region with lower atom density. We observe the deformation of the density defect into a linear shape. The linear shape is numerically reproduced and confirmed to be an array of linearly aligned four singly charged vortices. The motion of this density defect is explained as a combined motion of rotation and precession. Here the rotation means the motion of the defect around the center of the defect, whereas the precession means the motion of the defect around the center of the condensate as shown in the lower panel of Fig. 2(a) and the gray arrow in Fig. 2(b). Details of the figures are explained later. We confirm that an initial displacement of the multiply charged vortex is crucial to enable spontaneous splitting within an observation time both in the experiments and simulations. In fact, to reproduce the experimental observation, $r_{\text{ini}} = 0.2R_{\text{TF}}$ is required in the simulation, where R_{TF} is the Thomas-Fermi radius of the condensate.

A series of experiments was performed in order to study the vortex splitting [19]. We created a ^{87}Rb ($F = 2$, $m_F = 2$) BEC in an Ioffe-Pritchard magnetic trap. The number of atoms in the BEC was about 5×10^5 with a minimum magnetic field of $B_0 = 0.4$ G. The axial (radial) trapping frequency was $\omega_z = 2\pi \times 15$ Hz ($\omega_r = 2\pi \times 360$ Hz) and the axial (radial) Thomas-Fermi radius of the BEC was 60 μm (3 μm), and the chemical potential was 230 nK.

A quadruply charged vortex was topologically created in the BEC by reversing the axial magnetic field B_z from $B_0 = 0.4$ to -0.4 G in 3 ms [10]. In order to stabilize the formation of the vortex, a blue-detuned laser beam at the wavelength of 532 nm was applied below the BEC to remove the gravitational sag. To maintain axial confinement of the BEC after reversing the magnetic field, a red-detuned laser beam at the wavelength of 852 nm was focused at the condensate, which suppressed the axial expansion and the axial size of the BEC expanded from 160 to 240 μm during the holding time of 10 ms. In contrast, without the laser beam, the axial size of the BEC expanded from 170 to 550 μm. The time evolution of the vortex was observed using a tomographic imaging technique. We probed a 60 μm thick slice of the condensate axially, which was about one-third slice of the BEC for the time of flight (TOF) of 15 ms.

Images illustrating the time evolution of the density profile including the vortices are shown in Figs. 3(a)–3(d). Initially, the off-centered vortex precessed around the center of the BEC in the counterclockwise direction (a), which corresponds to the direction of the angular momentum. Then the deformation of the density defect was observed for the holding time of about 4.5 ms (b). This deformation into a linear shape could be held for a few ms [Figs. 3(c) and 3(d)]. For holding times longer than 7 ms, no vortices were clearly observed.

What is the cause of this linear deformation? We study the dynamics of the condensate using the time-dependent Gross-Pitaevskii (GP) equation $i\hbar\frac{\partial\phi(\mathbf{r},t)}{\partial t} = [-\frac{\hbar^2\nabla^2}{2m} + V(\mathbf{r}) + \frac{4\pi\hbar^2 a}{m}|\phi(\mathbf{r},t)|^2]\phi(\mathbf{r},t)$, where ϕ is the condensate wave function, V is the harmonic confinement potential, a is the s-wave scattering length, and m is the mass of a ^{87}Rb atom. To study small perturbations from multiply charged vortex states, we first consider its time-independent form $(-\frac{\hbar^2\nabla^2}{2m} - \mu + V + \frac{4\pi\hbar^2 a}{m}|\phi|^2)\phi = 0$. The wave function

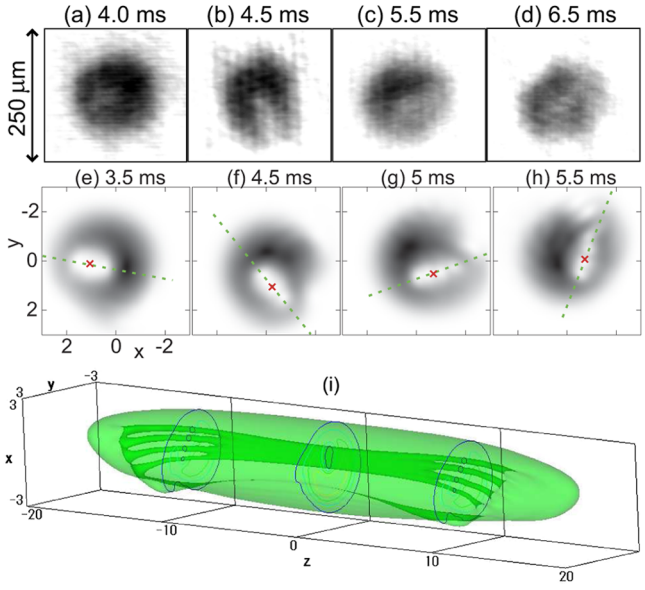

FIG. 3 (color online). (a)–(d) Axial absorption images of the BEC for the holding time of 4.0, 4.5, 5.5, and 6.5 ms. TOF = 15 ms. (e)–(i) 3D simulation using the time-dependent GP equation. Unit of length is μm. (e)–(h) Density profile, axially integrated over a central region (from -6.9 to 6.9 μm) at 3.5, 4.5, 5, and 5.5 ms. Dotted lines are operationally defined axes of the density defects. Crosses are the averages of positions of the vortices. (i) Density isosurface of the condensate at 3.5 ms for 5% of the maximum density. Contour lines at $z = 0, \pm 10$ μm are also plotted. Four split vortices are seen in the condensate.

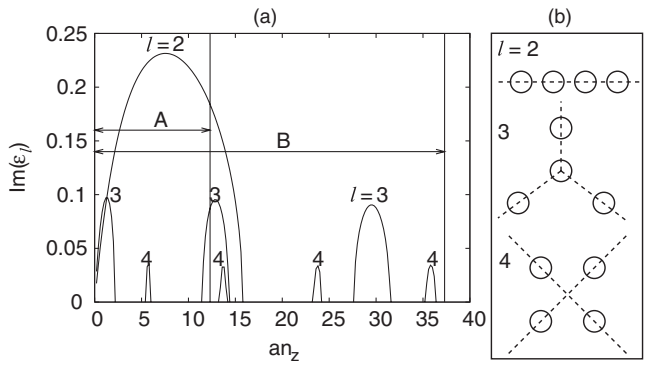

FIG. 4. (a) Quantum numbers $l = 2$, 3, and 4 show the existence of a complex excitation that causes the splitting in a two-, three-, or fourfold symmetric pattern at the linear density an_z, which is the same as that in Ref. [18]. The arrow A (B) is the range of an_z within a condensate of $N = 5 \times 10^4$ (2×10^5) atoms. Splitting with a twofold symmetry is dominant when $N = 5 \times 10^4$. (b) Splitting patterns of l-fold rotational symmetry. Circles represent singly charged vortices. Dotted lines are guides of symmetries.

can be written in the form $\phi = \sqrt{n}e^{i\varphi}$ where φ is the phase. The atom density n is zero along the vortex lines, and therefore vortices are associated with density defects. The velocity field $\frac{\hbar}{m}\nabla\varphi$ is proportional to the phase gradient. The wave function of a condensate with a quadruply charged vortex in a 2D rotationally symmetric system is of the form $\phi_0(r, \theta) = \phi_0(r)e^{i4\theta}$. A small perturbation to the initial condensate wave function is described by the eigenmodes of the Bogoliubov equations. In this system, the eigenfunctions for an eigenenergy ε_l can be written in the form $u_l(r)e^{i(l+4)\theta}$ and $v_l(r)e^{i(l-4)\theta}$, where l is the angular momentum index. Other indices are omitted.

The existence of complex eigenenergies is crucial for the splitting of multiply charged vortices through dynamical instability [14,15,18], because the population of such modes grows exponentially. They exist with indices $l =$ 2 to 6 in this model. Figure 4(a) shows the imaginary part of the eigenenergies for $l = 2$, 3, 4 for the range of an_z relevant for the present experimental setup, where n_z is a linear atom density [20], which corresponds to the interaction parameter η for the 2D system in Ref. [18]. The arrow A in Fig. 4(a) represents the range of an_z for a condensate with 5×10^4 atoms, which is roughly the number of atoms in the present experiment. Within this range, the $l = 2$ splitting mode is dominant since it has the largest imaginary part of the eigenenergy in a wide range of an_z. When only the lth mode is excited, the perturbed wave function has the form $\phi(r, \theta, t) = e^{i4\theta}\{\phi_0(r) + [u_l(r)e^{il\theta}e^{-i\varepsilon_l t/\hbar} + v_l^*(r)e^{-il\theta}e^{i\varepsilon_l t/\hbar}]\}$. The periodicity of the θ-dependent factors means that the contribution from an excitation with index l makes the density of the condensate to be l fold rotationally symmetric. Therefore the splitting pattern must have l-fold symmetry. Figure 4(b) is a sketch of two-, three-, and fourfold rotationally symmetric patterns of singly charged vortices.

A numerical simulation using the 3D time-dependent GP equation was performed to study the dynamics. In our simulation, we assume a cigar-shaped condensate of 5×10^4 ^{87}Rb atoms confined in a harmonic trap with radial and axial trapping frequencies of 360 Hz and 36.6 Hz, respectively, which mimics our experimental setup. Corresponding to the experimental results in Figs. 3(a)–3(d) which are not rotationally symmetric, we used an asymmetric initial condition in which the quadruply charged vortex is displaced by $r_{\text{init}} = 0.2R_{\text{TF}}$ from the center of the trap. The classification of splitting patterns using the rotational symmetry remains valid even in this asymmetric system, because the patterns come from quantized phase changes of wave functions around the vortex core.

The result of the simulation shows that the quadruply charged vortex splits into four parallel vortices, as shown in Fig. 3(i). The splitting pattern is the same within the whole condensate. Figures 3(e)–3(h) are images of the density, axially integrated from $z = -6.9$ to 6.9 μm, corresponding to the experimentally observed central one-third of the condensate taken with the tomographic imaging technique. The main feature of our experiment, which is the deformation into the linear shape, is successfully reproduced in the simulation. We performed additional numerical simulations of the TOF process and verified that positions of

the vortices relative to the condensate and the pattern symmetry of the vortices are conserved.

Detailed look into the behavior of the linear defect consisting of vortices shows a combined motion of "rotation" and "precession" both in the experiment, Figures 3(a)–3(d), and the simulation, Figs. 3(e)–3(h). We define the axis of the linear defect and the average position of the vortices as shown in Figs. 3(e)–3(h) as dashed lines and crosses, respectively. Change of the angle of this axis is rotation and the change of the angle of the average position relative to the trap center is precession.

This combined motion can be understood by a velocity field [12]. We assume a condensate with a TF density profile in a model 2D system. To understand the rotational motion, we must consider the fact that each of the four singly charged vortices make a velocity field $v_\theta(r) = \frac{\hbar}{mr}$, where r is the distance from the vortex core. Each vortex follows the velocity field produced by the other three vortices. The sum of velocities causes the rotation of the defect, as illustrated in Fig. 2(a). If all of the vortices are separated by a distance d, the period of rotation is $\frac{2\pi m}{\hbar} d^2$ (inner pair of vortices) and $\frac{9}{11} \frac{2\pi m}{\hbar} d^2$ (outer pair). To understand the precession, for each vortex at a radius r_i, we introduce an antivortex at a radius R_{TF}^2/r_i, in order to have the particle flow velocity at the surface of the condensate parallel to the surface [12], as shown in Fig. 2(b). The velocity field of these image vortices causes the precession of the original vortices. If all the vortices were at the same place $r_i = 0.2R_{\mathrm{TF}}$, the period was $\frac{2\pi m}{\hbar} R_{\mathrm{TF}}^2 0.24$. In general, the distance between vortices is $d \lesssim R_{\mathrm{TF}}$, and therefore, the periods of rotation and precession have a similar time scale. From Fig. 3(a) to 3(b), it is seen that the periods of both the precession and the rotation are about 2 ms in the experiment. The axis of the defect passes the center of the condensate there, while it does not in Fig. 3(c). It means that the rotational velocity slightly exceeds precessional one. The aforementioned periods of the rotation $\frac{2\pi m}{\hbar} d^2$ (inner pair) and $\frac{9}{11} \frac{2\pi m}{\hbar} d^2$ (outer pair) also become about 2 ms when $d = 0.5$ μm. In the simulation, the periods of rotation and precession are about 3 and 4 ms, respectively. These periods from the experiment, simplified model, and the simulation reasonably match each other.

We also checked these behaviors with different initial displacements $r_{\mathrm{init}} = 0.05$ to $0.15R_{\mathrm{TF}}$ in the simulation. The linear alignment of the vortex cores was reproduced also in these cases. The distances between the vortices are, however, much smaller and the density defect does not reach the edge of the condensate. To reproduce the experimental observation, $r_{\mathrm{init}} \simeq 0.2R_{\mathrm{TF}}$ is required. Therefore we estimate that the initial displacement in the experiment is around $0.2R_{\mathrm{TF}}$. In our experiment, the vortex displacement observed at $t = 0$ is smaller. Oscillation of the condensate during the formation of the vortex possibly causes additional displacement after the observation at $t = 0$. Also, the existence of the $m_F = +1$ component possibly affects the displacement observed at $t = 0$ although it is not confirmed due to noise in the observations.

In a condensate with a larger number of atoms, see arrow B in Fig. 4(a), the twofold splitting should be dominant only at the ends (where $an_z < 15$), and the other splitting should appear near the center of the condensate. Our 3D simulation for a condensate of 2×10^5 atoms supports these expectations. Therefore, it is possible to control the symmetry of the splitting pattern by controlling the number of atoms.

T. I. is supported by the JSPS and J. H. by the Finnish Cultural Foundation. This work was supported by MATSUO Foundation, the Grant-in-Aid for Scientific Research (Grants No. 13740255, No. 16540357, No. 18043013, and No. 18204035), and SCOPE-S, and the Grant-in-Aid for the 21st century COE "Center for Diversity and Universality in Physics" from the Ministry of Education, Culture, Sports, Science and Technology (MEXT) of Japan.

[1] P. Nozières and D. Pines, *The Theory of Quantum Liquids* (Addison-Wesley, Redwood City, CA, 1990).
[2] E. J. Yarmchuk, M. J. V. Gordon, and R. E. Packard, Phys. Rev. Lett. **43**, 214 (1979).
[3] M. R. Matthews *et al.*, Phys. Rev. Lett. **83**, 2498 (1999).
[4] A. L. Fetter and A. A. Svidzinsky, J. Phys. Condens. Matter **13**, R135 (2001).
[5] R. Blaauwgeers *et al.*, Nature (London) **404**, 471 (2000).
[6] M. Baert *et al.*, Phys. Rev. Lett. **74**, 3269 (1995).
[7] V. Penna, Phys. Rev. B **59**, 7127 (1999).
[8] A. Leanhardt *et al.*, Phys. Rev. Lett. **89**, 190403 (2002).
[9] Y. Shin *et al.*, Phys. Rev. Lett. **93**, 160406 (2004).
[10] M. Kumakura *et al.*, Phys. Rev. A **73**, 063605 (2006).
[11] M. F. Andersen *et al.*, Phys. Rev. Lett. **97**, 170406 (2006).
[12] C. J. Pethick and H. Smith, *Bose Einstein Condensation in Dilute Gases* (Cambridge University Press, Cambridge, England, 2002).
[13] E. Lundh, Phys. Rev. A **65**, 043604 (2002); K. Kasamatsu, M. Tsubota, and M. Ueda, Phys. Rev. A **66**, 053606 (2002); U. R. Fischer and G. Baym, Phys. Rev. Lett. **90**, 140402 (2003).
[14] H. Pu *et al.*, Phys. Rev. A **59**, 1533 (1999).
[15] M. Möttönen *et al.*, Phys. Rev. A **68**, 023611 (2003).
[16] A. M. Mateo and V. Delgado, Phys. Rev. Lett. **97**, 180409 (2006).
[17] J. Huhtamäki *et al.*, Phys. Rev. Lett. **97**, 110406 (2006).
[18] Y. Kawaguchi and T. Ohmi, Phys. Rev. A **70**, 043610 (2004).
[19] M. Okano *et al.*, J. Low Temp. Phys. **148**, 447 (2007).
[20] $n_z = \int n(x, y, z)dxdy$, where n is the atom density.